



# Primary Frequency Regulation by Demand Side Response

Ibrahim M. Alotaibi<sup>1</sup> · M. A. Abido<sup>1,2</sup> · M. Khalid<sup>1,2</sup>

Received: 12 August 2020 / Accepted: 3 February 2021 / Published online: 20 February 2021  
© King Fahd University of Petroleum & Minerals 2021

## Abstract

Recently, there have been growing attempts to replace conventional power generators with renewable energy sources. However, the inertia reduction that results from such measures jeopardizes the stability of the power system. Typically, power system operators utilize the spinning generating units to provide the required capacity to preserve system frequency where the carbon emission and wear/tear costs considerably affect their feasibility. Instead, this paper investigates the ability to use the existing assets (i.e., controllable demands) in providing the regulation needed to maintain the frequency within the allowable ranges. The proposed study reveals that the dynamically controlled space heaters were able to provide a fast primary response without a significant impact on the regular operation of the heaters. The proposed approach successfully reduced the conventional generator's regulating capacity during a sudden loss of generation/or a sudden increase in demand. Highlighting the impact of inertia reduction on the overall performance concludes the proposed study.

**Keywords** Ancillary services · Controllable demands · Demand side response · Frequency regulation · Space heaters · Genetic algorithm

## List of symbols

$C$	Heat capacity (kJ/kg K)
$D$	Percentage of frequency sensitive loads (%)
$E$	The energy in (MWh)
$H$	Generator inertia (s)
$K$	Lead-lag gain
$M_{\text{air}}$	Mass of air (kg/m <sup>3</sup> )
$M_{\text{dot}}$	Air mass flow (kg/h)
$P_L$	Load power (MW)
$P_e$	Electric power (MW)
$P_m$	Mechanical power (MW)
$P_v$	Valve power (MW)
$R$	Droop characteristic constant
$R_{\text{eq}}$	Building thermal resistance (k/W)
$T_1$	Lead-lag controller time constant (s)
$T_2$	Lead-lag controller time constant (s)
$T_T$	Turbine time constant (s)
$T_{\text{amb}}$	Ambient temperature $F$
$T_g$	Governor time constant (s)

$T_{\text{indoor}}$	Indoor temperature $F$
$T_{\text{in}}$	Temperature reference $F$
$T_{\text{room}}$	Room temperature $F$
$\frac{dQ}{dt}$	Heat flow
$\Delta f$	Frequency deviation in (p.u.)
$\Delta T$	Temperature difference in $F$
$\Delta\omega$	Speed deviation in (p.u.)

## 1 Introduction

In an AC power grid, the imbalance between generation and demand and the increased penetration of renewable energy resources (RESs) that are inherently intermittent possess a significant threat to system stability. Power system stability can be defined as the ability of the system to regain the state of equilibrium after being subjected to a disturbance. When system frequency gets altered, the governor adjusts its action given its droop characteristics, aiming to restore the equilibrium state. If, for instance, the supply and demands are not balanced due to a substantial loss of a generating unit, a sudden change in demands, and fluctuations in renewables, the frequency may rapidly change [1–4]. Frequency response services are provided to maintain the frequency within the allowable range limits [ $\pm 0.1$ Hz] [5]. A sudden drop in frequency is usually

✉ Ibrahim M. Alotaibi  
Alotaibi.ib@gmail.com

<sup>1</sup> Electrical Engineering Department, King Fahd University of Petroleum and Minerals, Dhahran 31261, Saudi Arabia

<sup>2</sup> K.A. CARE Energy Research and Innovation Center, Dhahran, Saudi Arabia



contained by primary response actions that should be responsive within (1 s–20 s) [2]. However, bringing back system frequency to its typical operating point requires secondary frequency responsive actions that may take (30 s–30 min). If the previous actions were taken and yet the frequency keeps declining, further interventions (i.e., load shedding) should be performed to prevent the system from collapsing. Naturally, all large generating units (i.e., 100 MW capacity) are required to provide mandatory frequency response services [2]. Partially loaded generators may be deployed to provide the required capacity to balance the sudden offset in generation-load balance.

Recently, there have been growing interests in the deployment of controllable demands to provide the required frequency response services. The existing assists of flexible demands can be used to reduce the needs for a primary response from the generators that are partially loaded, thereby the operating costs and CO<sub>2</sub> emissions are reduced. Such measures would also incentivize the consumers to participate in providing frequency responsive services by bidding their available controllable capacities in a deregulated electricity market. A quick survey carried out in the Scopus database [6] revealed that a total of 287 documents had been uploaded in the engine to address the utilization of demand response (DR) in frequency regulation applications. The majority were published in 2018, indicating the research trend in that field. On the other hand, energy storage systems (ESSs) may facilitate renewables' integration by adjusting their energy behavior [7]. ESSs can be classified based on their functions and storage forms, as indicated in [8–10]. There are broad devices utilized in high power applications such as flywheels (FESS), supercapacitors, and specially configured batteries in terms of functions. In contrast, large-scale batteries, compressed air energy storage, and flow batteries are commonly operated in energy management applications [3, 11–13]. Although the ESSs cost has been rapidly decaying (Thanks to the electric vehicles), they remain expensive, and their deployment needs to be carefully studied. For instance, a 20 MW/10 MWh Flywheel storage may cost approximately \$100 m to \$110 m [14]. Controllable demands or aggregated demand response (DR) may act as a virtual energy storage systems. Intelligent management of DR's power and energy consumption may result in functions similar to those provided by typical energy storage devices. In addition, the smart utilization of the existing assets will provide the required ancillary services with much lesser cost. For instance, aggregated refrigerators with a total capacity of [20 MW] would cost \$15m compared to the FESS, which costs \$100m to \$110m of the same capacity [14]. DR has the potential to reduce the ESS market share by 50% in 2030 [12]. However, the utilization of DR introduces uncertainty in response, and simultaneous disconnection or connection to the loads may lead to frequency drop/rise,

causing further instability issues. Such behavior will be considered in the proposed control scheme.

The rest of the paper is structured as follows: Sect. 2 presents an extensive literature review on the relevant publications that have been reported so far. The mathematical models are presented in Sect. 3. The results and discussions are delivered in Sect. 4. The concluding remarks and future work are summarized in Sect. 5. The derived state-space models are provided in the “Appendix.”

## 2 Related Work

The high penetration of renewable energy sources (RESs) such as solar PV or wind energy systems, which are increasingly replacing conventional power generators, leads to a reduction in the system's total inertia. Such reduction exposes the frequency of the system to unwanted variations. Therefore, virtual synchronous machines (VSMs) were proposed in [15–20] to mimic the inertial behavior of conventional synchronous generators. A synchronous virtual machine that mimics the inertial behavior of conventional generators to provide frequency regulation services was proposed in [15]. The characteristics of the weak grid were addressed through the modeling of VSM. The performance of the grid was investigated for different levels of injections using batteries and ultracapacitors. A virtual inertia-based load modulation strategy was developed in [16] to offset the frequency deviation caused by the uncertainties of renewable energy resources. Different scenarios were considered to examine the proposed studies. A benchmark of an IEEE 39 bus was used to validate the proposed scheme. The authors of [19] proposed a conventional power system model appended with individually–collaboratively DR and virtual inertial-model for the purpose of frequency regulation and control. The proposed energy protocol allows power operators to combine/ choose all/among those services to provide the action needed if the frequency deviation occurs. On the other hand, the authors of [20] proposed a coordinated control strategy for an islanded microgrid based on primary frequency signaling. The presented study aims to coordinate the ESS and RES, given the source limitations based on the droop method and virtual impedance.

In a deregulated electricity market, consumers are encouraged to participate in power grid ancillary services to improve system resiliency. Moreover, data centers (DC) usually exploit load elasticity to help to maintain the load-generation balance. However, the responsive time of data centers is relatively slow, limiting the ability to provide real-time support. To mitigate such an issue, the authors of [21] proposed a coupled DC-battery to provide fast frequency regulating capabilities. The coordination succeeded in reducing the battery size needed compared to a stand-alone



system, while the authors of [22] presented a study that assesses the financial performance of a BESS to provide market-based frequency regulation services. The potential impact on profitability was also highlighted and evaluated. Naturally, the replacement of bulky conventional generators by renewables results in an inertial mass reduction, which jeopardizes grid stability. Therefore, the authors of [3] proposed a coordinated control scheme to effectively operate a hybrid system composed of ultra-capacitor and batteries for ancillary services purposes in the electricity market.

Ancillary services can be provided by smart control strategies to the existing assets in the network, such as dispersed energy storage systems [23–27]. For instance, the authors of [23] proposed a virtual energy storage system (VESS) that consisted of controllable demands and flywheel storage system (FSS) to provide power system ancillary services. Feasibility studies were carried out to validate the benefits of deploying such protocols over conventional measures. A hybrid ultra-capacitor and battery storage systems were proposed in [24] to provide extensive scale regulation services. The proposed scheme aims to mitigate the excessive utilization of the battery if deployed to provide such ancillary services and increase regulation services' profitability. Moreover, the authors of [25] used a vanadium-redox flow battery-based energy device model to provide multi-ancillary services focusing on peak-shaving application and frequency support. A cooperative dynamic energy level balancing based on consensus control among distributed energy storage devices offering frequency regulation capabilities in a droop-controlled microgrid was investigated in [26]. A combined heat and power microgrid based on heat pumps and energy storage system coordinated control strategy was presented in [27] to smooth tie-line power fluctuations.

Frequency regulation services can also be provided by proper adjustments to the power consumption of the controllable devices [28–37]. For example, the authors of [28] proposed a control algorithm for dynamically controlled refrigerators to provide primary frequency control services in Great Britain. Similarly, the authors of [29] investigated the ability of dynamically controlled loads to maintain grid frequency within a particular range post a sudden loss of generation. The proposed study indicates a significant delay in frequency fall and less reliance on rapidly deployable backup generators. The authors of [30] used aggregated controlled bitumen tanks to provide sufficient reserve capacity for frequency support applications. The model was found reliable and faster in response compared to a frequency-sensitive generating units. In addition, the authors [31] investigated the potential range of average power that can be offered by electric water heaters if adequately controlled for power balancing applications. The control strategy was achieved by adjusting the setpoint temperature and the drawn water. A methodology to support grid frequency and voltage profile

by using a controllable load consisting of an electric water heater and electric vehicles was presented in [32]. The availability of domestic refrigerators and industrial bitumen tank load to provide frequency response services was investigated in [33]. Recently, a coordinated control strategy of Inverter-based air-conditioning (IAC) and fixed air-conditioning is proposed in a grid that is dominated by renewable energy sources to provide primary frequency regulation [38]. In the primary frequency response, the regulating capacity is provided by adjusting the setpoints of the air-conditioning units. Moreover, a recovery method is also proposed to restore the initial operating states of the IAC after regulation. The proposed study is concluded by verifying its effectiveness on a six-machine two-area system and an isolated microgrid.

A decentralized controllable protocols were proposed in [34, 39, 40]. In [34], the authors proposed a two-layer control algorithm for thermostatically controllable loads to effectively participate in fast frequency regulation services due to the scarcity of AGCs in a microgrid that is highly penetrated by RESs. Also, a relatively recent study proposed in [38] presents a novel thermo-electrical dynamic that is based on reproducing the dynamical models of air conditioners ACs and ground source heat pumps GSHPs, along with an existing model of electric water heaters EWHs to improve a decentralized demand response strategy for direct load control (DLC) for providing primary frequency regulation in hybrid isolated microgrids. Different cases are analyzed to demonstrate the effectiveness of the proposed control scheme. Furthermore, Reference [40] proposed aggregated electric vehicles to provide a centralized supplementary frequency regulation through a mediator between the demands and the power system control center considering the charging requirements. A decentralized controller was also proposed to adjust load power consumption in proportion to grid frequency.

The state-of-the-art in demand response (DR) applications in the modern power system have been reviewed by [37, 41–43]. The role of demand-side response in frequency regulation applications was investigated in [41]. The authors highlighted the centralized and decentralized control strategies that are adopted to mitigate the generation-load mismatch in the power grid. The authors concluded the article by indicating the future direction in demand-side control applications. The authors of [42] have presented an architecture testbed for providing demand response (telemetric monitoring and actuation of loads) for frequency support applications. The authors of [43] have extended the previous work by reviewing the potential challenges and new control schemes of frequency control in the modern power system. For instance, in [37], the authors have investigated the participation of demand response control loops for different load variations. The authors have utilized linear matrix inequalities to coordinate between the DR and secondary

control loop to minimize the frequency deviation due to communication delays.

However, instead of using numerous electrical appliances to provide the required ancillary services, few large load centers such as local malls are used, thereby minimizing the response time and the control loops. This paper proposes a novel control scheme that uses the thermal space heaters of distinctive large centers in providing the primary frequency regulation services by adjusting their power consumption. A lead-lag controller with its optimized parameters using real coded genetic algorithm (RCGA) is incorporated into the system to enhance the overall response. The paper also proposes a very efficient control scheme that considers consumers’ comfort and heaters’ inherent characteristics to limit switching cycles and indoor temperatures. Highlighting the impact of inertia reduction on the behavior of the frequency concludes the proposed study.

### 3 Problem Definition

#### 3.1 Power System Model

Consider the power system model shown in Fig. 1 for the proposed study. The details of the simplified power system model can be found in the “Appendix” [44].

#### 3.2 Generator Model

A small perturbation is applied on the swing equation of a synchronous machine given by (1) yields:

$$\frac{2H}{\omega_s} \frac{d^2 \Delta \delta}{dt^2} = \Delta P_m - \Delta P_e \tag{1}$$

$$\frac{d\Delta\left(\frac{\omega}{\omega_s}\right)}{dt} = \frac{1}{2H} (\Delta P_m - \Delta P_e) \tag{2}$$

With speed expressed in per unit, Eq. (2) becomes as follows:

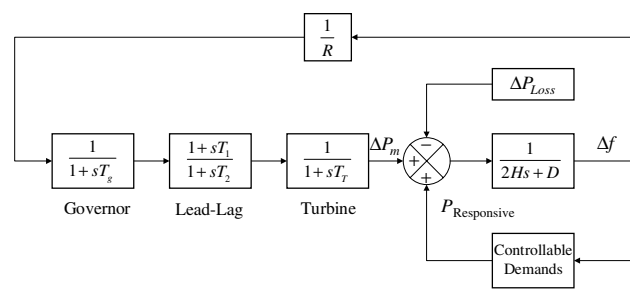


Fig. 1 Simplified power system model

$$\frac{d\Delta\omega}{dt} = \frac{1}{2H} (\Delta P_m - \Delta P_e) \tag{3}$$

Taking the Laplace transform leads to:

$$\Delta\Omega(s) = \frac{1}{2Hs} [\Delta P_m(s) - \Delta P_e(s)] \tag{4}$$

#### 3.3 Load Model

The load in the power system may consist of insensitive and sensitive components. Heating and lighting loads are considered non-sensitive loads, while motors are frequency-dependent loads. The speed-load characteristics of a composite load may be approximated as follows:

$$\Delta P_e(s) = \Delta P_L(s) + D\Delta\omega(s) \tag{5}$$

The term  $D\Delta\omega$  indicates the frequency-dependent load where  $\Delta P_L$  refers to the non-sensitive loads.  $D$  is expressed as the percentage change in load over the deviation of frequency.

#### 3.4 Prime Mover Model

A prime mover whose energy is generated through the burning of gas, coal, and nuclear fuel can be approximated by (6). The model relates the change in steam valve position  $\Delta P_V(s)$  to the changes in mechanical power output  $\Delta P_m(s)$ .

$$G_p(s) = \frac{\Delta P_m(s)}{\Delta P_V(s)} = \frac{1}{1 + s\tau_T} \tag{6}$$

#### 3.5 Governor Model

If the electrical load is suddenly increased, the generator’s electrical power exceeds the mechanical power, which causes the machine to spin slower. The change in speed is sensed by the governor, which immediately acts to adjust the turbine input aiming to bring the speed to a new steady state operating point. The speed governor may act as a comparator whose output  $\Delta P_g$  is the difference between the reference power  $\Delta P_{ref}$  and the power  $\frac{1}{R}\Delta\omega$  resulted from the speed characteristic of the governor. i.e.,

$$\Delta P_g(s) = \Delta P_{ref}(s) - \frac{1}{R} \Delta\Omega(s) \tag{7}$$

where  $R$  is the slope of the governor speed characteristics (i.e., the change in speed over the change in power). The command  $\Delta P_g$  is transformed via the hydraulic amplifier to the steam valve position  $\Delta P_V$ . Under the assumption of a linear relationship and considering a time constant  $\tau_g$ .

$$\Delta P_v(s) = \frac{1}{1 + s\tau_g} \Delta P_g(s) \tag{8}$$

### 3.6 Space Heater of a Building

The thermal models given by (9) through (11) are used to describe the heat transfer processes in a building [45–47]. The following parameters were taken into consideration when building the dynamical models in the Simulink environment.

- House geometry
- Thermal properties
- The thermal resistance of the house
- Heater characteristics
- Initial temperatures

Model components are:

- Reference Temperature (Desired Setpoint)
- A thermostat that considers the temperature variations
- The heater has a constant airflow rate
- The heat flow into the room, which is governed by (9):

$$\frac{dQ}{dt} = (T_{\text{Heater}} - T_{\text{Room}}) \times M_{\text{dot}} \times C \tag{9}$$

Where  $T_{\text{heater}}$  is the temperature of the hot air from the heater and  $T_{\text{Room}}$  refers to the room temperature.  $\frac{dQ}{dt}$  represents the heat flow from the heater into the room.  $M_{\text{dot}}$  is the air mass flow rate, and  $C$  indicates the heat capacity of the air. The house model constitutes room temperature variations, heat flow from the heater, and heat losses to the environment. The heat losses and the temperature rate of change are governed by:

$$\left(\frac{dQ}{dt}\right)_{\text{Losses}} = \frac{1}{Req} \times (T_{\text{Room}} - T_{\text{out}}) \tag{10}$$

$$\frac{dT_{\text{Room}}}{dt} = \frac{1}{M_{\text{air}} \times C} \times \left(\frac{dQ_{\text{heater}}}{dt} - \frac{dQ_{\text{Losses}}}{dt}\right) \tag{11}$$

where  $M_{\text{air}}$  refers to the mass of air inside the house in  $\frac{\text{kg}}{\text{m}^3}$ .  $Req$  represents the thermal resistance of a house in  $\frac{\text{K}}{\text{W}}$ .

### 3.7 Lead-Lag Controller Design

A lead-lag controller whose transfer function is given by (12) is introduced into the system to effectively achieve a steady state error reduction and simultaneous reduction of overshoot and rise time of the system response. A Real

Coded Genetic Algorithm (RCGA) was used to allocate the optimal parameters of the controller.

$$K \frac{1 + sT_1}{1 + sT_2} \tag{12}$$

where  $K$  and  $T_1, T_2$  are the gain and time constants of the controller, respectively.

### 3.8 Real Coded Genetic Algorithm

A real coded genetic algorithm (RCGA) with the parameters shown in Table 1 was developed to allocate the optimal parameters of the controller incorporated with the power system model. The derivation of the state space model and equivalent transfer functions utilized in this paper is provided in the ‘‘Appendix.’’

### 3.9 Proposed Control Scheme

The adjustable current demands are deployed to participate in primary frequency response instead of the generator. Unlike the proposed approaches in the literature that utilize a large number of appliances to achieve primary frequency support, four large loads (e.g., local malls) are considered to carry out the analysis. The mall temperature setpoints, comfort, and maximum switches per hour of the heaters are taken into account while designing the control algorithm.

If the space heaters switching cycles are assumed to be within the range of [1–8] per hour. The switching actions caused by the primary frequency response that lasts 30 s should not disturb space heaters’ regular operation [29]. The US Department of Energy (DoE) report on smart grid applications provides typical latency values. For instance, the report estimated that the typical latency for demand response applications is in the range of [500 ms to 2 s], which is faster than the conventional generators’ action that takes [10 s] to provide the same task [48, 49]. Also, today’s latency is expected to be much lower than the reported values due to the tremendous communication infrastructure advancements.

A simplified layout that summarizes the workflow of the controller structure is shown in Fig. 2. The upper part presents the power system model. Generally, the synchronous

Table 1 RCGA parameters

Parameter	Value
Population	40
Generations	100
BLX $\alpha$	0.5
Crossover probability	0.7
Mutation probability	0.05

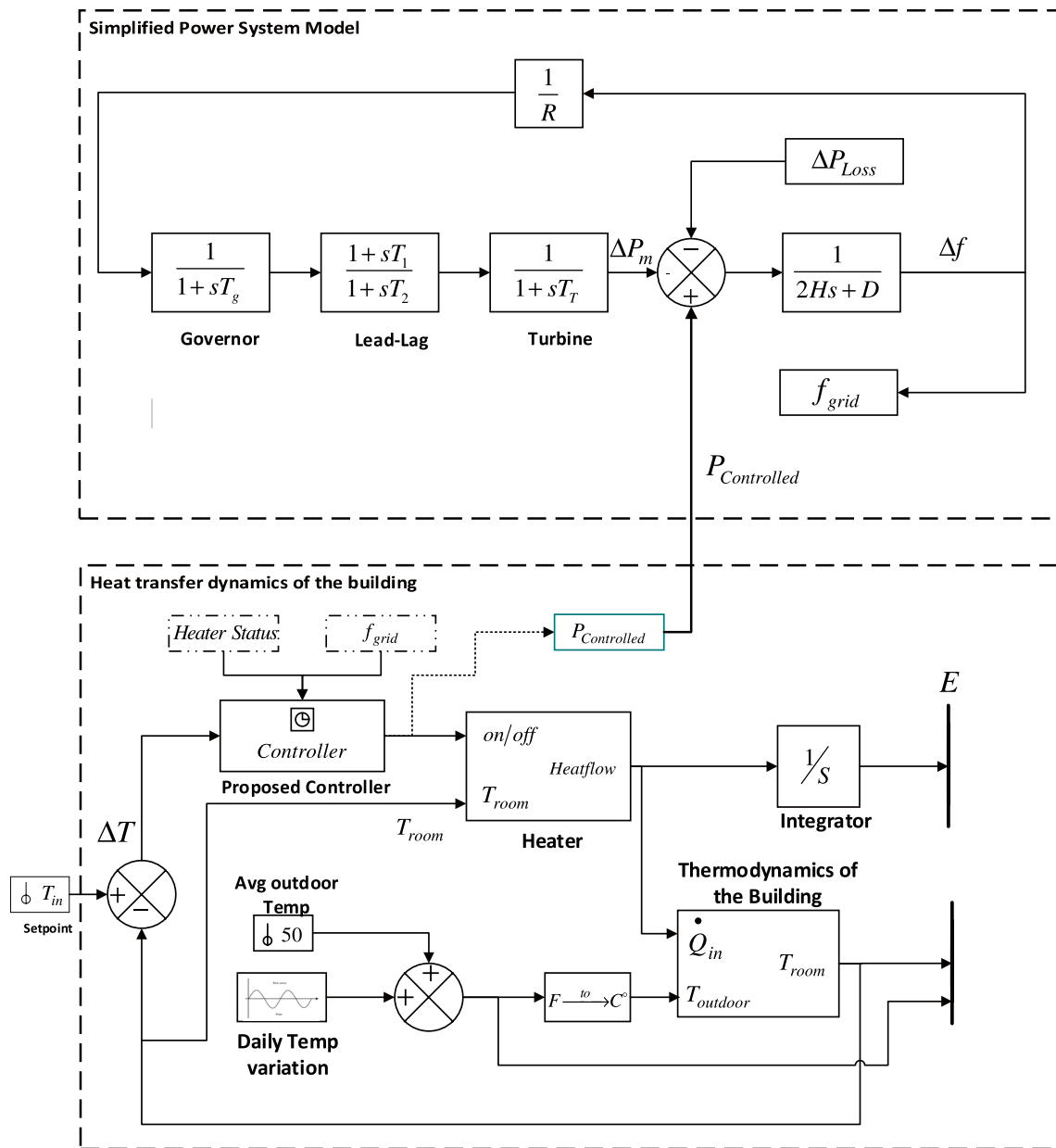


Fig. 2 Controller structure

generators meet the primary frequency requirements that are mechanically coupled to the turbine and the governor. The governor senses and measures the frequency deviation and generates the necessary control signal to the turbine. The turbine acts accordingly by increasing or decreasing the mechanical power to sustain the mismatch. Such a process can be viewed as a Proportional control loop. However, the above control loop is modified to accommodate the proposed control scheme.

On the other hand, the lower part shows the structure of the building’s thermodynamics and the space heater. Typically, a thermostat compares the indoor temperature with

the setpoints  $[T_{Low}, T_{High}]$  and hence produces the triggering signal to the heater. If the indoor temperature is above  $T_{High}$ , the heater is switched off, whereas if the indoor temperature falls below  $T_{Low}$ , the heater is switched on. The controller is designed such that it receives four inputs. That is, the indoor temperature, grid frequency, heater status, and the maximum number of switches. Furthermore, the controller is required to consider the heater status since the ON heaters are allowed to be switched off if the frequency drops, and the OFF heaters are triggered if the grid frequency rises. The controller is allowed to operate as long as the indoor temperature is within the dead-band. Simultaneous switching

is not permissible as such action may even lead to further instability issues. Different temperature setpoints are considered for the sake of demand diversity.

## 4 Results and Discussion

### 4.1 Power System Model in Simulink

The mathematical models described in the above sections (i.e., 0 through 1.5) are developed in the Simulink. A step-change in the load was applied to the system to observe the frequency deviation. The system response due to such an increase in the load is shown in Fig. 3. The steady state error was relatively high, and such behavior needs to be adjusted. The countermeasure to adjust the deviation of the frequency will be treated in the upcoming sections. The values of  $[T_g, T_T, H, D, R]$  are  $[0.2 \text{ s}, 0.5 \text{ s}, 5 \text{ s}, 0.8 \text{ p.u.}, 0.05 \text{ p.u.}]$ , respectively [28, 29, 44].

### 4.2 Power System Model

A sudden loss of generation/or a sudden increase in demand  $[0.2 \text{ p.u.}]$  was applied to the simplified power system model depicted in Fig. 1. Such disturbance resulted in approximately 0.863 Hz deviation from the nominal frequency of 60 Hz. The response of the system needs to be damped to reduce the overshoot and rise time. Therefore, a lead-lag controller is integrated to enhance the response of the system.

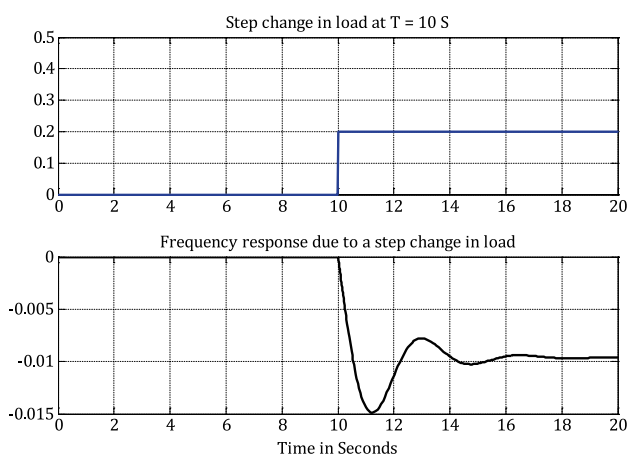


Fig. 3 System’s frequency deviation due to a sudden increase in the demand

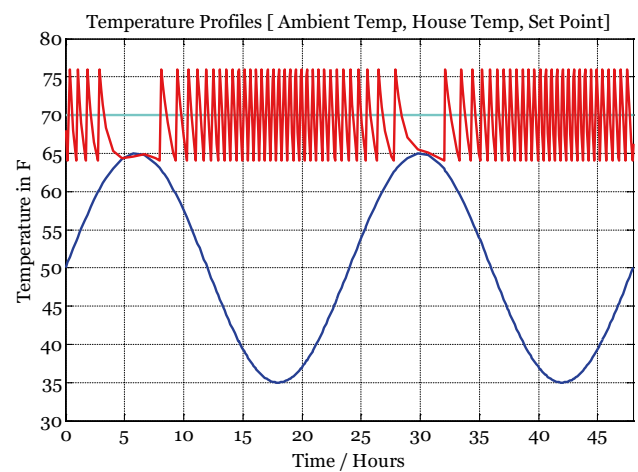


Fig. 4 Temperature profiles of the building and ambient and setpoint

### 4.3 Space Heating Model of a Big Load Center

Figure 4 shows the temperature profile of the building and the ambient temperature. The indoor temperature was allowed to vary within a  $[\mp 10 \text{ F}]$ , while the ambient temperature varied sinusoidally. The setpoint was kept constant for the entire simulation period.

### 4.4 Proposed Control Approach

Figure 5 depicts the response of the system with multiple scenarios. Before the disturbance, the units were operating normally. However, once the disturbance was applied, the controller disconnected the units whose temperature setpoints were within their dead-band, starting by the lowest. The proposed control approach successfully reduced the frequency deviation when a sudden increase in the demand

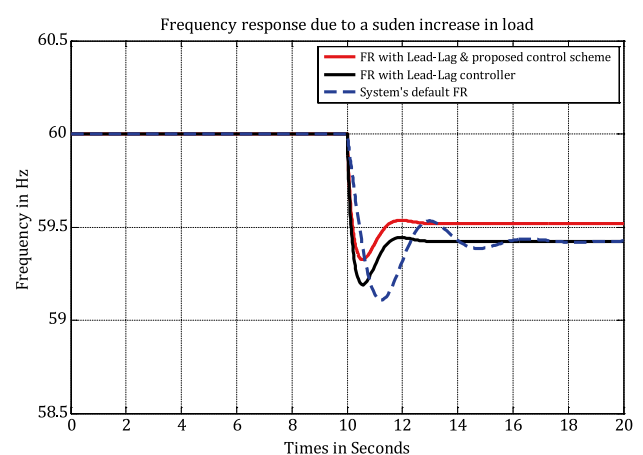
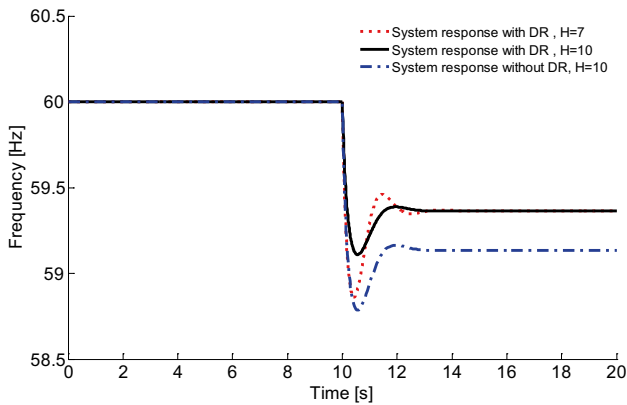


Fig. 5 System response with lead-lag controller and proposed control scheme

**Table 2** Time response characteristics

	Metric	P-Controller	Proposed controller
1	$f_{final}$ (Hz)	59.423	59.654
2	Settling time (s)	18.570	12.249
3	Rise time (s)	0.283	0.306
4	% Overshot	0.971	0.580
5	Min $f$ (Hz)	58.946	59.552

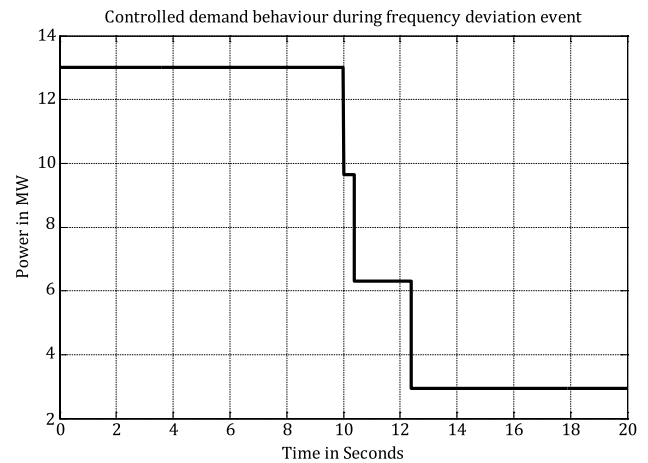


**Fig. 6** Impact of inertia reduction on the overall performance

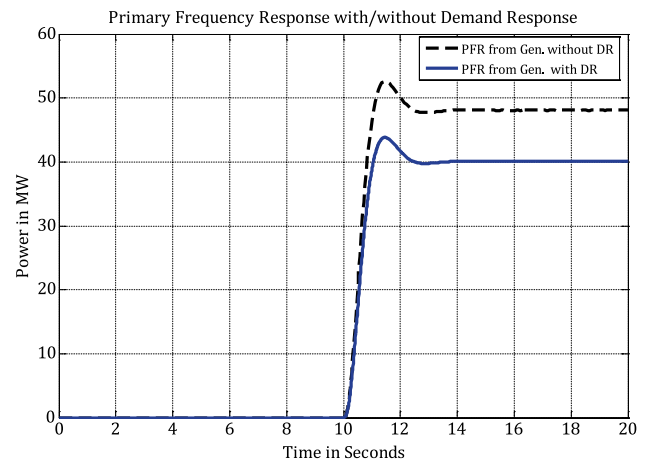
took place at  $[t = 10 \text{ s}]$ . The system natural response and the controlled response are shown in the same figure. The proposed control scheme clearly shows an outstanding performance since it arrested the minimum frequency deviation (i.e., frequency nadir). Also, due to the suggested control scheme, the steady state frequency landed into a new narrower operating point (i.e., 59.6 Hz) versus (59.4 Hz).

Table 2 addresses the time response characteristics of the conventional controller (i.e., Proportional controller) and the proposed control strategy. It is seen from table that the proposed controller succeeded in stabilizing the frequency into a better steady state value compared to the proportional controller. It is also seen that the proposed strategy achieved a significant reduction in the settling time. Furthermore, the percentage of overshoot indicates the superiority of the proposed control layout over the conventional approach.

The impact of inertia reduction is shown in Fig. 6. Clearly, the decrease in inertia constant due to the high penetration of smart and renewable resources deteriorates the system response if subjected to unforeseen disturbances. Although the proposed control scheme is not designed to mitigate the inertial reduction, the frequency nadir under the suggested control layout was reduced, suggesting a positive impact on the overall transient response. On the other hand, Fig. 7



**Fig. 7** Demand behavior during the instant of losing 0.2 p.u. of generation



**Fig. 8** Generator response in primary frequency response timeframe

shows the demand variation due to the sudden increase in load. As pointed out earlier, simultaneous connection and disconnection to the flexible loads are not permitted as such behavior may furtherly deteriorate the system’s stability.

Figure 8 compares the primary response of the conventional generator during the instant of losing [0.2 p.u.] generation/or a sudden increase in demand. In addition, the response depicted in Fig. 8 compares the amount of power required from the generator to provide the primary frequency service with/and without the proposed control approach. The amount of the supplied power from the synchronous generator after the disturbance was reduced due to the aggregated power supplied by the controllable loads, indicating that the space heaters successfully provided the system with its ancillary services requirements and reduced the reliance on conventional generators to arrest the frequency.



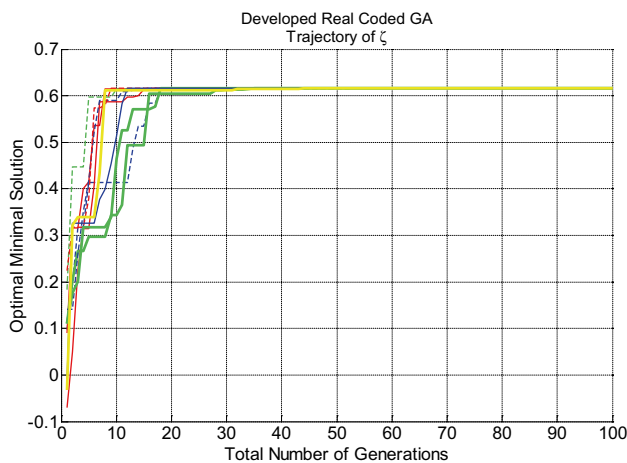
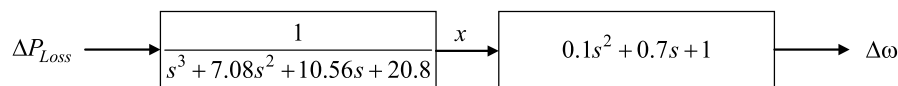


Fig. 9 Damping trajectory by RCGA

### 4.5 Real Coded Genetic Algorithm

A real coded genetic approach with the parameters shown in Table 1 is developed to maximize the damping coefficient  $\zeta$  to enhance the response of the system. A lead-lag controller was incorporated, its optimal parameters were obtained by the developed RCGA. Figure 9 shows the maximum damping coefficient attained during the simulation. The optimal parameters for the controller are listed in Table 3.



### 5 Conclusion

Dynamically controlled space heaters were successfully developed in the Simulink environment. An aggregated model that represents several large industrial loads was incorporated with a simplified power system model aiming to participate in ancillary services requirements. A real coded genetic algorithm to allocate the lead-lag controller parameters for enhancing the overall response was developed. Different setpoints were assumed to maintain load diversity and to examine the feasibility of the

Table 3 Optimal controller parameters

Parameter/ $\zeta$	Optimal value
$\zeta$	0.62
$K$	1
$T_1$	0.47
$T_2$	0.1

proposed control strategy. The proposed control scheme indicated that the dynamically controlled space heaters were able to provide fast primary frequency response without a significant impact on the regular operation of the heaters. The proposed approach succeeded in reducing the regulating capacity needed from the conventional generator during a sudden increase in demand/or sudden loss of generation. The presented study also highlighted the impact of inertia reduction on the transient response with/without demand-side participation. The existing assets can be extended to include dispersed energy storage systems in the distribution system to participate in ancillary services.

### Appendix

#### Key Parameters of the Power System Model

See Table 4.

#### Closed Loop Uncontrolled Matrix

$$x \times (s^3 + 7.08s^2 + 10.56s + 20.8) = \Delta P_{Loss} \tag{13}$$

$$\begin{bmatrix} \dot{x}_1 \\ \dot{x}_2 \\ \dot{x}_3 \end{bmatrix} = \begin{bmatrix} 0 & 1 & 0 \\ 0 & 0 & 1 \\ -20.8 & -10.56 & -7.08 \end{bmatrix} \begin{bmatrix} x_1 \\ x_2 \\ x_3 \end{bmatrix}$$

Table 4 Power system data

Parameter	Value
Inertia constant $H$ in (s)	5
Turbine time constant $T_1$ in (s)	0.5
Governor time constant $T_g$ in (s)	0.2
Governor droop characteristic $R$ (p.u.)	0.05
Damping coefficient $D$	0.8
Power step change $\Delta P$ (p.u.)	0.2

## Closed Loop Matrix with Lead-Lag Controller

$$\frac{\Delta\omega}{\Delta P} = \frac{K_2 \left( \frac{1+sT_1}{1+sT_2} \right) + \left( \frac{1}{10s+0.8} \right)}{K_1 \left( \frac{1}{1+0.2s} \right) \left( \frac{1}{1+0.5s} \right) \left( \frac{1}{10s+0.8} \right) \left( \frac{1+sT_1}{1+sT_2} \right) K_2 + 1} \quad (14)$$

$$\begin{aligned} & x[0.8 + K_1 K_2 + s(10.56 + 0.8T_2 + K_1 K_2 T_1) \\ & + s^2(7.08 + 10.56T_2) + s^3(7.08T_2 + 1) + s^4T_2] \\ & = \Delta P_{Loss} \end{aligned} \quad (15)$$

$$\begin{bmatrix} \dot{x}_1 \\ \dot{x}_2 \\ \dot{x}_3 \\ \dot{x}_4 \end{bmatrix} = \begin{bmatrix} 0 & 1 & 0 & 0 \\ 0 & 0 & 1 & 0 \\ 0 & 0 & 0 & 1 \\ \frac{-(0.8+K_1K_2)}{T_2} & \frac{-(10.56+0.8T_2+K_1K_2T_1)}{T_2} & \frac{-(7.08+10.56T_2)}{T_2} & \frac{-(7.08T_2+1)}{T_2} \end{bmatrix}$$

**Acknowledgments** The authors would like to acknowledge the support provided by King Fahd University of Petroleum & Minerals through the Direct Funded Project No. DF191004. Dr. Abido would also like to acknowledge the funding support provided by K.A. CARE Energy Research and Innovation Center (ERIC), KFUPM. The authors also acknowledge Qassim University for their continuous support.

## References

- Shafiullah, M.; Rana, M.J.; Abido, M.A.: Power system stability enhancement through optimal design of PSS employing PSO. In 2017 4th International Conference on Advances in Electrical Engineering (ICAEE), pp. 26–31 (2017). <https://doi.org/10.1109/ICAEE.2017.8255321>
- Samarakoon, K.; Ekanayake, J.; Jenkins, N.: Investigation of domestic load control to provide primary frequency response using smart meters. *IEEE Trans. Smart Grid* **3**(1), 282–292 (2012). <https://doi.org/10.1109/TSG.2011.2173219>
- Akram, U.; Khalid, M.: A coordinated frequency regulation framework based on hybrid battery-ultracapacitor energy storage technologies. *IEEE Access* **6**, 7310–7320 (2018). <https://doi.org/10.1109/ACCESS.2017.2786283>
- Alam, A.; Abido, M.A.: Parameter optimization of shunt FACTS controllers for power system transient stability improvement. In: 2007 IEEE Lausanne Power Tech, pp. 2012–2017 (2007). <https://doi.org/10.1109/PCT.2007.4538627>
- SEC: The Saudi Arabian Grid Code. Saudi Electricity Company (SEC), KSA, Issue 01, May 2007
- ELSEVIER: Scopus—Document search. <https://www.scopus-com.extoljp.kfupm.edu.sa/search/form.uri?display=basic>. Accessed November 21, 2018
- Tungadio, D.H.; Sun, Y.: Load frequency controllers considering renewable energy integration in power system. *Energy Rep.* **5**, 436–453 (2019). <https://doi.org/10.1016/j.egy.2019.04.003>
- Rohit, A.K.; Devi, K.P.; Rangnekar, S.: An overview of energy storage and its importance in Indian renewable energy sector: part I—technologies and comparison. *J. Energy Storage* **13**, 10–23 (2017). <https://doi.org/10.1016/j.est.2017.06.005>
- Chen, H.; Cong, T.N.; Yang, W.; Tan, C.; Li, Y.; Ding, Y.: Progress in electrical energy storage system: a critical review. *Prog. Nat. Sci.* **19**(3), 291–312 (2009). <https://doi.org/10.1016/j.pnsc.2008.07.014>
- Gustavsson, J.: Energy storage technology. *Energy Storage Symposium*. Available <http://adsabs.harvard.edu/abs/1976enst.symp...54L> (1976)
- Ramírez, M.; Castellanos, R.; Calderón, G.; Malik, O.: Placement and sizing of battery energy storage for primary frequency control in an isolated section of the Mexican power system. *Electr. Power Syst. Res.* **160**, 142–150 (2018). <https://doi.org/10.1016/j.epsr.2018.02.013>
- Cheng, M.; Sami, S.S.; Wu, J.: Benefits of using virtual energy storage system for power system frequency response. *Appl. Energy* **194**, 376–385 (2017). <https://doi.org/10.1016/j.apenergy.2016.06.113>
- Canevese, S.; Gatti, A.; Micolano, E.; Pellegrino, L.; Rapizza, M.: Battery energy storage systems for frequency regulation: simplified aging evaluation. In: 2017 6th International Conference on Clean Electrical Power (ICCEP), Santa Margherita Ligure, Italy, pp. 291–297 (2017). <https://doi.org/10.1109/ICCEP.2017.8004830>
- Drysdale, B.; Wu, J.; Jenkins, N.: Flexible demand in the GB domestic electricity sector in 2030. *Appl. Energy* **139**, 281–290 (2015). <https://doi.org/10.1016/j.apenergy.2014.11.013>
- Bose, U.; Chattopadhyay, S.K.; Chakraborty, C.; Pal, B.: A novel method of frequency regulation in microgrid. *IEEE Trans. Ind. Appl.* **55**(1), 111–121 (2019). <https://doi.org/10.1109/TIA.2018.2866047>
- Delavari, A.; Kamwa, I.: Virtual inertia-based load modulation for power system primary frequency regulation (2018). <https://doi.org/10.1109/PESGM.2017.8274601>
- Fang, J.; Li, H.; Tang, Y.; Blaabjerg, F.: Distributed power system virtual inertia implemented by grid-connected power converters. *IEEE Trans. Power Electron.* **33**(10), 8488–8499 (2018). <https://doi.org/10.1109/TPEL.2017.2785218>
- Fang, J.; Li, X.; Tang, Y.; Li, H.: Power management of virtual synchronous generators through using hybrid energy storage systems (2018). <https://doi.org/10.1109/APEC.2018.8341201>
- Saeed Uz Zaman, M.; Bukhari, S.B.A.; Hazazi, K.M.; Haider, Z.M.; Haider, R.; Kim, C.-H.: Frequency response analysis of a single-area power system with a modified LFC model considering demand response and virtual inertia. *Energies* (2018). <https://doi.org/10.3390/en11040787>
- Wu, D.; Guerrero, J.M.; Vasquez, J.C.; Dragicevic, T.; Tang, F.: Coordinated power control strategy based on primary-frequency-signaling for islanded microgrids (2013). <https://doi.org/10.1109/ECCE.2013.6646817>
- Guruprasad, R.; Murali, P.; Krishnaswamy, D.; Kalyanaraman, S.: Coupling a small battery with a datacenter for frequency regulation. (2018). <https://doi.org/10.1109/PESGM.2017.8274094>
- Avendano-Mora, M.; Camm, E.H.: Financial assessment of battery energy storage systems for frequency regulation service. In: 2015 IEEE Power Energy Society General Meeting (2015). <https://doi.org/10.1109/PESGM.2015.7286504>
- Cheng, M.; Sami, S.S.; Wu, J.: Virtual energy storage system for smart grids. **88**, 436–442 (2016). <https://doi.org/10.1016/j.egypr.2016.06.021>
- Kim, Y.; Raghunathan, V.; Raghunathan, A.: Design and management of battery-supercapacitor hybrid electrical energy storage systems for regulation services. *IEEE Trans. Multi-Scale Comput. Syst.* **3**(1), 12–24 (2017). <https://doi.org/10.1109/TMSCS.2016.2627543>
- Lucas, A.; Chondrogiannis, S.: Smart grid energy storage controller for frequency regulation and peak shaving, using a vanadium redox flow battery. *Int. J. Electr. Power Energy Syst.* **80**, 26–36 (2016). <https://doi.org/10.1016/j.ijepes.2016.01.025>
- Morstyn, T.; Hredzak, B.; Agelidis, V.G.: Distributed cooperative control of microgrid storage. *IEEE Trans. Power Syst.* **30**(5),



- 2780–2789 (2015). <https://doi.org/10.1109/TPWRS.2014.2363874>
27. Wang, R., et al.: A coordination control strategy of battery and virtual energy storage to smooth the micro-grid tie-line power fluctuations. *Zhongguo Dianji Gongcheng Xuebao Proceedings Chin Soc. Electr. Eng.* **35**(20), 5124–5134 (2015). <https://doi.org/10.13334/j.0258-8013.pcsee.2015.20.002>
  28. Wu, J.; Hung, W.; Ekanayake, J.; Jenkins, N.; Coleman, T.; Cheng, M.: Primary frequency response in the great britain power system from dynamically controlled refrigerators. In: 22nd International Conference and Exhibition on Electricity Distribution (CIRED 2013), Stockholm, Sweden, pp. 0507–0507 (2013). <https://doi.org/10.1049/cp.2013.0772>
  29. Short, J.A.; Infield, D.G.; Freris, L.L.: Stabilization of grid frequency through dynamic demand control. *IEEE Trans. Power Syst.* **22**(3), 1284–1293 (2007). <https://doi.org/10.1109/TPWRS.2007.901489>
  30. Cheng, M., et al.: Power system frequency response from the control of bitumen tanks. *IEEE Trans. Power Syst.* **31**(3), 1769–1778 (2016). <https://doi.org/10.1109/TPWRS.2015.2440336>
  31. Elamari, K.; Lopes, L.A.C.; Tonkoski, R.; Using electric water heaters (EWHs) for power balancing and frequency control in PV-diesel hybrid mini-grids, pp. 842–850 (2011). <https://doi.org/10.3384/ecp11057842>
  32. Tokudome, M.; Tanaka, K.; Senjyu, T.; Yona, A.; Funabashi, T.; Kim, C.-H.: Frequency and voltage control of small power systems by decentralized controllable loads. In: 2009 International Conference on Power Electronics and Drive Systems (PEDS), Taipei, Taiwan, pp. 666–671 (2009). <https://doi.org/10.1109/PEDS.2009.5385834>
  33. Cheng, M.; Wu, J.; Galsworthy, S.; Jenkins, N.; Hung, W.: Availability of load to provide frequency response in the great Britain power system. In: 2014 Power Systems Computation Conference, pp. 1–7 (2014). <https://doi.org/10.1109/PSCC.2014.7038294>
  34. Yao, Y.; Zhang, P.; Wang, Y.: A two-layer control method for thermostatically controlled loads to provide fast frequency regulation. *Zhongguo Dianji Gongcheng Xuebao Proceedings Chin Soc. Electr. Eng.* **38**(17), 4987–4998 (2018). <https://doi.org/10.13334/j.0258-8013.pcsee.171181>
  35. Yan, S.; Wang, M.-H.; Yang, T.-B.; Hui, S.Y.R.: Instantaneous frequency regulation of microgrids via power shedding of smart load and power limiting of renewable generation. Presented at the ECCE 2016—IEEE Energy Conversion Congress and Exposition, Proceedings (2016). <https://doi.org/10.1109/ECCE.2016.7855207>
  36. Pourmousavi, S.A.; Nehrir, M.H.: Real-time central demand response for primary frequency regulation in microgrids. *IEEE Trans. Smart Grid* **3**(4), 1988–1996 (2012). <https://doi.org/10.1109/TSG.2012.2201964>
  37. Bharti, K.; Singh, V.P.; Singh, S.P.: Impact of intelligent demand response for load frequency control in smart grid perspective. *IETE J. Res.* (2020). <https://doi.org/10.1080/03772063.2019.1709570>
  38. Jiang, I.; Ju, P.; Wang, C.; Li, H.; Liu, J.: Coordinated control of air-conditioning loads for system frequency regulation. *IEEE Trans. Smart Grid*, pp. 1–1 (2020). <https://doi.org/10.1109/TSG.2020.3022010>
  39. Mendieta, W.; Cañizares, C.A.: Primary frequency control in isolated microgrids using thermostatically controllable loads. *IEEE Trans. Smart Grid*, pp. 1–1 (2020). <https://doi.org/10.1109/TSG.2020.3012549>
  40. Liu, H.; Hu, Z.; Song, Y.; Wang, J.; Xie, X.: Vehicle-to-grid control for supplementary frequency regulation considering charging demands. *IEEE Trans. Power Syst.* **30**(6), 3110–3119 (2015). <https://doi.org/10.1109/TPWRS.2014.2382979>
  41. Malik, A.; Ravishankar, J.: A review of demand response techniques in smart grids. Presented at the 2016 IEEE Electrical Power and Energy Conference, EPEC 2016 (2016). <https://doi.org/10.1109/EPEC.2016.7771745>
  42. Thornton, M.; Motalleb, M.; Smidt, H.; Branigan, J.; Siano, P.; Ghorbani, R.: Internet-of-things hardware-in-the-loop simulation architecture for providing frequency regulation with demand response. *IEEE Trans. Ind. Inform.* **14**(11), 5020–5028 (2018). <https://doi.org/10.1109/TII.2017.2782885>
  43. Obaid, Z.A.; Cipcigan, L.M.; Abraham, L.; Muhssin, M.T.: Frequency control of future power systems: reviewing and evaluating challenges and new control methods. *J. Mod. Power Syst. Clean Energy* (2018). <https://doi.org/10.1007/s40565-018-0441-1>
  44. Saadat, H.: *Power Systems Analysis*, 3rd edn. McGraw-Hill, New York (2010)
  45. Balan, R.; Donca, R.; Balan, A.; Ple, A.: Thermal modelling and temperature control of a house. *Romanian Rev. Precis. Mech. Opt. Mechatron.* **39**, 4 (2011)
  46. Källblad, K.: Thermal models of buildings. *lund Inst. Technol.* **80** (1998)
  47. Thavlov, A.; Bindner, H.W.: Thermal Models for Intelligent Heating of Buildings. *Proc. Int. Conf. Appl. Energy ICAE*, p. 11 (2012)
  48. M. Donnelly, D.J.; Trudnowski, S. M., Dagle, J.E.: Autonomous demand response for primary frequency regulation. *PNNL-21152*, 1118120 (2012). <https://doi.org/10.2172/1118120>
  49. Zeinali, M.; Thompson, J.S.: Practical evaluation of UK internet network characteristics for demand-side response applications. In: 2018 IEEE International Conference on Communications, Control, and Computing Technologies for Smart Grids (Smart-GridComm), pp. 1–6 (2018). <https://doi.org/10.1109/SmartGridComm.2018.8587541>

